Frequency Identification for the Pulsating White Dwarf GD358

Anicia Arredondo *Center for Astrophysics, Space Physics and Engineering Research at Baylor University*

Dr. Dwight Russell *Department of Physics at Baylor University*

Richard Campbell *Department of Mechanical Engineering at Baylor University*

***Abstract*—The pulsating white dwarf GD358 was observed three times during June 2014 at Paul and Jane Meyer Observatory as part of observations for the Whole Earth Telescope collaboration. The image processing software Astro-ImageJ was used for photometry analysis of the raw images, and the resulting lightcurves were used in Mathematica for determination of the frequencies of the vibrational modes. The measured frequencies were compared to values measured from longer runs of data given on the Whole Earth Telescope Website. The project was successful in finding these frequencies, but a larger amount of data would be beneficial for obtaining more refined results.**

I. Introduction

White dwarfs are the ending life state of the large majority of stars, including our sun [1]. Because the evolution of white dwarf stars depends only on cooling and not fusion, white dwarfs are easier to model than younger stars [2]. The rate of cooling of white dwarfs can be used to determine the composition of the core, and to predict birth rates of the stars [3]. Not all white dwarfs pulsate, but the ones that do can be studied by asteroseismology, the study of a pulsating star's frequency spectra. These spectra are used in order to better understand the interiors of pulsating white dwarfs, and to learn more about stellar life cycles.

The varying luminosity of white dwarf stars is caused by non-radial gravity wave pulsations within the star [1] [4] [5]. Pulsations are very short, on the order of 100 to 1000 seconds, allowing for a large amount of data in a short time span [6] [5]. In order to get more continuous data, the Whole Earth Telescope (WET) has one to two week long periods where several observatories around the world observe the same star at staggering times. This allows for a continuous stream of data by ensuring that when one observatory stops observations for the night another one begins where the first left off. A longer span of data allows for a more accurate measurement of vibrational frequencies [4].

During the summer of 2014 the Paul and Jane Meyer Observatory (PJMO) participated in the latest WET observing run of the variable white dwarf GD358. GD358 is a DBV white dwarf, which means it has an effective temperature around 25,000k and an atmosphere made up of mostly Helium [7].

This paper reports three nights of GD358 data from that run. The software Astro-ImageJ was used for photometry analysis, and Mathematica was used to plot the frequency spectra and pinpoint the most prominent frequencies. The goal of this project was mainly to contribute data to WET, but also to accurately measure frequencies that can be compared to the values given on the WET website [8].

II. Theory

The frequencies of pulsation of a white dwarf can be calculated by doing a discreet Fourier transform on the measured amplitudes of the star [6]. First, the measured amplitudes must be corrected for DC offset, which we do by subtracting the average of all points from each individual point. This ensures that the Fourier transform will be done on the varying amplitudes of the data and not on a large window spectrum that significantly drowns out the data [9].

The formula for a discreet Fourier transform is given in Equation (1) where N is the total number of points, u_r is the number of counts at point r, and s is related to frequency. We apply this formula to all measured amplitudes.

$$X(s) = \frac{1}{\sqrt{N}} \sum_{r=1}^{N} u_r \, e^{\frac{2\pi i (r-1)(s-1)}{N}} \qquad (1)$$

In order to plot X(s), a time step between each point must be estimated. From Equation (1) it can be deduced that frequency is proportional to s. The frequency step, ΔF, can be calculated from the time between images, Δt, using Equation (2) where T is the total time for the observing run.

$$\Delta F = \frac{1}{N\Delta t} = \frac{1}{T + \Delta t} \quad (2)$$

A plot of ΔF vs X(s) can now be made. This is the frequency spectrum of the star. From this plot, frequencies that should correspond to normal modes of vibration can be determined.

It is useful to note that a larger T will give a smaller ΔF, which will result in higher resolution of the frequency spectrum. With a smaller ΔF, we are able to see that there is fine structure splitting in each peak, and we are therefore able to pick out more frequencies [10]. An example of this fine structure splitting can be seen in Fig. 1. Splitting can be seen most prominently in the 1223μHz and 1245μHz peaks. What could have been interpreted as one peak in the bottom graph is actually two in the top graph, and with more observations and a smaller ΔF those peaks could become 3 or more. The purpose of WET is to refine these frequencies to a level of precision that is impossible for one observatory to do alone.

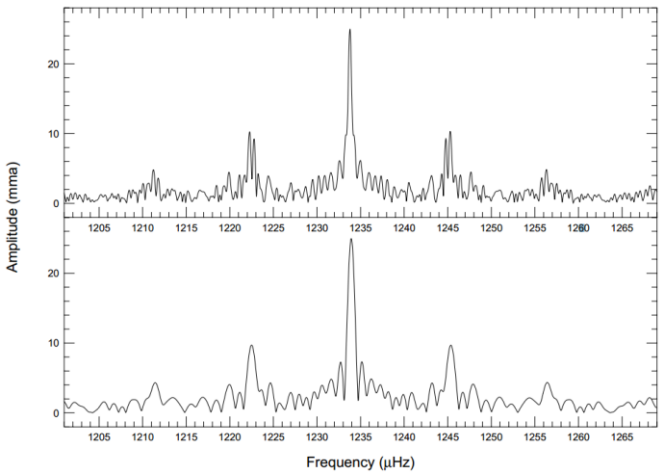

Fig. 1. The top graph shows the fine structure splitting in data that can be seen when observed for a longer time frame. The bottom graph shows the same data observed for a shorter time frame, where the time span is significantly shorter.

III. Observations

GD358 was observed on three different nights from PJMO using a ST-10XE CCD Camera with a 2×2 binned detector attached to a 0.61 meter Ritchey-Chretien cassegrain telescope with an f/9 focal length. The image scale is 1.96 pixels per arc second and the field of view is 9.29×6.26 arc minutes. Because the observations were a part of the larger WET run, there was no need to choose a target star. Data was obtained for as long as possible on any given night, and observations were only stopped for weather disruptions or the beginning of astronomical twilight.

GD358 is a fairly bright star with a magnitude of 13.65, so all images were taken at 20 second exposures through a BG40 filter. On each night we also imaged bias frames, dark frames, and flat frames in order to correct for instrumental errors caused by the mechanics of the camera.

Fair amounts of data were obtained from the first two nights, and neither night had any complications. There is a large gap in the data from the third night which was caused by a malfunction with the telescope's camera. The camera's cooling system went offline, causing it to forcibly turn off and stop imaging. It was brought back online, but 25% of the data from that night was lost because the failure was not immediately noticed and it took a significant amount of time for the camera to return to the temperature needed for imaging. Because a Fourier transform cannot be applied to non-continuous data, the data from the third night is treated as two separate observations during analysis.

IV. Method

Astro-ImageJ was used for instrumental corrections to the raw science images and to output a lightcurve and table of measurements of time and relative flux of GD358. In order to ensure that the measured signal is the true signal from the target and background stars, bias, dark and flat field corrections must be applied to the images. Fig. 2 shows the effect of applying these corrections.

A bias frame is an image taken at a 0 second exposure time with the camera shutter closed. A bias allows us to reduce the noise caused by the camera itself [11]. On each night, 30 bias frames were taken and averaged to make a master bias image, and the master bias is subtracted from the raw images.

A dark frame is an image taken at the same exposure as the target images and it is also taken with the shutter closed. This is a way to correct for thermal noise caused by the electric current that flows through the pixels on the CCD chip of the camera. It is important to cool the camera down to -35º before taking dark frames, because then the movement of atoms is slowed and there is less thermal noise. 30 frames were taken,

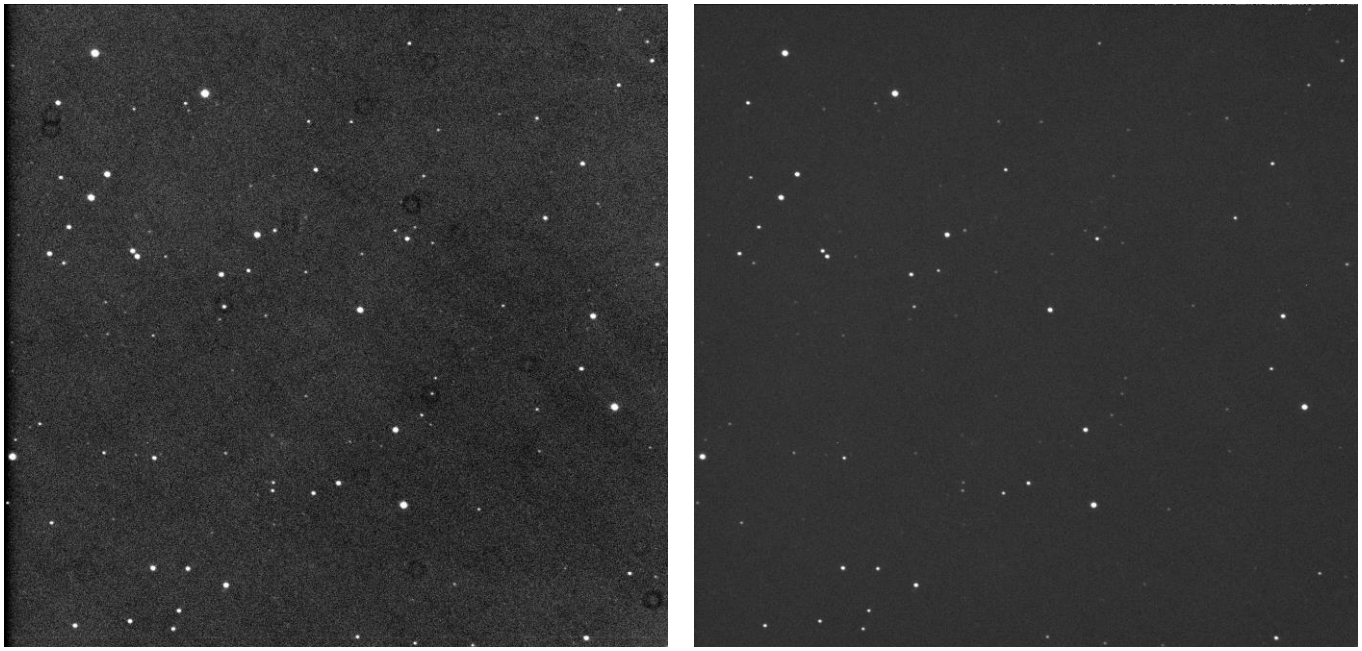

Fig. 2. The image on the left shows the star field used to observe GD358 and comparator stars before instrumental corrections were made. Notice the grey hue of the image, the black line on the left edge, and the ring shapes scattered throughout the field. The image on the right shows the same star field after applying biases, darks, and flats. The contrast is improved and the black line and ring shapes are eliminated.

averaged and subtracted from the raw images.

A flat field is 10 second exposure of a homogeneously illuminated background, and is used to compensate for variations in pixel sensitivity within the CCD chip and to remove shadows caused by dust and other foreign substances that fall onto the CCD chip and block the image. 30 flat frames were taken and normalized by averaging all 30 together and dividing by the average pixel counts of one single image. The normalized master flat is then divided out of the raw images.

Once Astro-ImageJ was done with instrumental corrections, it began to do the photometry on the target object as well as 2 other comparator stars. The purpose of comparator stars is to correct for discrepancies in data caused by clouds or other irregularities by subtracting the averaged comparator signal from the target signal. The counts of each object minus the counts of the sky background were measured and plotted against time. Also included in the graphs were error in the measurement of the target's flux, a plot of airmass vs time, and a plot of sky background vs time. Each curve has been scaled and vertically shifted in order to be able to see all curves on a single graph.

In addition to the light curve, Astro-ImageJ produced a table of measurements for all objects including relative flux, error, signal to noise ratio, and total signal counts. The most important parts of the table for this project are the values for relative flux of the target at specific times, which can be used to estimate frequencies by applying a discreet Fourier transform to the data.

The time given in the table was converted from reduced Julian days to seconds, and the relative flux values were altered to account for the DC window offset. A Fourier Transform was applied to the values for the relative flux, and they were paired with estimations of the frequency that were calculated from time using Equation (2). Graphs of frequency vs. amplitude were plotted in Mathematica, and values for the frequencies of vibrational modes were estimated by recording the value for frequency at the each peak in the spectra. This is a very tedious job, as each spectrum could have thirty or more peaks in it. Therefore only peaks with amplitudes of more than 0.02 were recorded.

Many of the identified peaks were discovered to be combinations of two or more modes, especially when the frequencies were measured to be 2000μHz or more. If a measured frequency was close to two different known modes, the median was taken and the measured value was paired with whichever mode it was closer to.

V. RESULTS

Fig. 2 and Fig. 3 show the measured lightcurves from the first two nights of data. Fig. 4 shows the lightcurve from the third night, including the gap which was caused by the failure

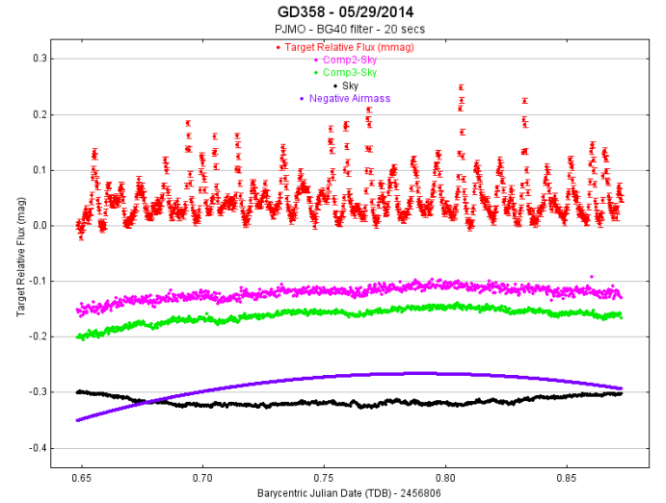

Fig.2. Lightcurve from the 4.45 hours observed on the first night. 20 second exposures were made through a BG40 filter. The red curve is GD358, the pink and green curves are the comparator stars, the black curve is sky background, and the purple curve is airmass.

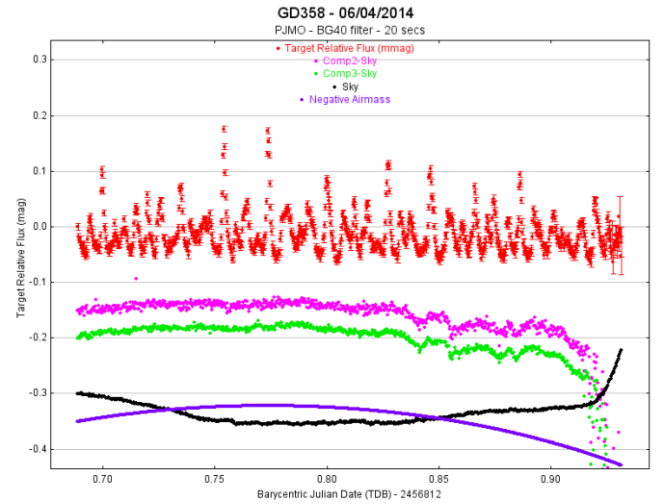

Fig.3. Lightcurve from the 5.84 hours observed on the second night. 20 second exposures were made through a BG40 filter. The red curve is GD358, the pink and green curves are the comparator stars, the black curve is sky background, and the purple curve is airmass. The drop off at the end was caused by incoming clouds, which terminated the observing run.

of the camera. Though the gap is large, it is still usable for frequency analysis. Fig. 5 shows the resulting frequency plots for the three nights of data, where the third night was split into two separate data sets.

Frequencies were successfully identified from four sets of power spectra, and a summary of the results as compared to the values given on the WET website is given in Table 1. Most of the F-mode frequencies were identified with less than 2% error. If a measured frequency differed from the published value by more than 2%, it was not included in the table.

Unfortunately, the F1, F4 or F7 frequencies were not identifiable from any of the three nights of data. This is most

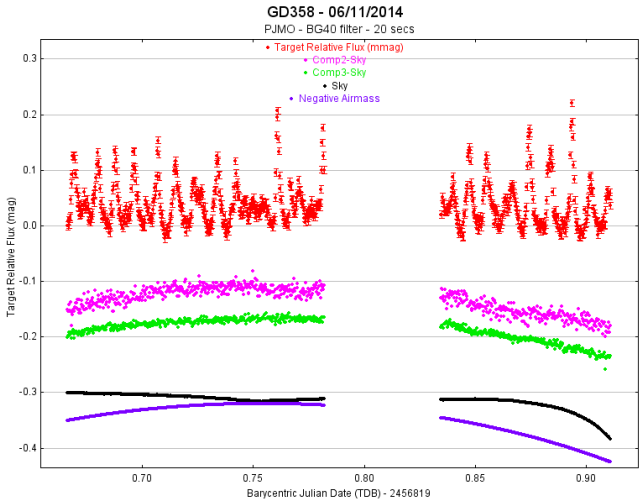

Fig.4. Lightcurve from the 5.88 hours observed on the first night, including the 1.3 hour gap where the camera failed. 20 second exposures were made through a BG40 filter. The red curve is GD358, the pink and green curves are the comparator stars, the black curve is sky background, and the purple curve is airmass.

likely because our relatively short imaging time was not sufficient enough to refine the peaks well enough to tell the difference between the three separate frequencies. From Table 1 we can see that the published values of F1, F7 and F10 are remarkably close to each other, which is evidence for the existence of splitting and explains the fact that this project was unable to identify an F1 or F7 peak.

TABLE I
MEASURED FREQUENCY MODES

Mode	Published Frequency (μHz)	Observed Value (μHz)	Percent Error
F11	2534.7	2534	0.0
F5	2366.8	2397	1.3
F8	2362.7	2345	0.7
F6	2358.8	2340	0.7
F3	2158.6	2156	0.1
F2	1735.9	1723	0.7
F4	1229.0		
F9	1247.8	1251	0.3
F7	1236.3		
F1	1235.2		
F10	1233.5	1217	1.3
F12	1149.7	1168	1.6

Table 1 gives a summary of results as compared to the frequencies given on the WET website. A blank space means a comparable value for that mode was not found.

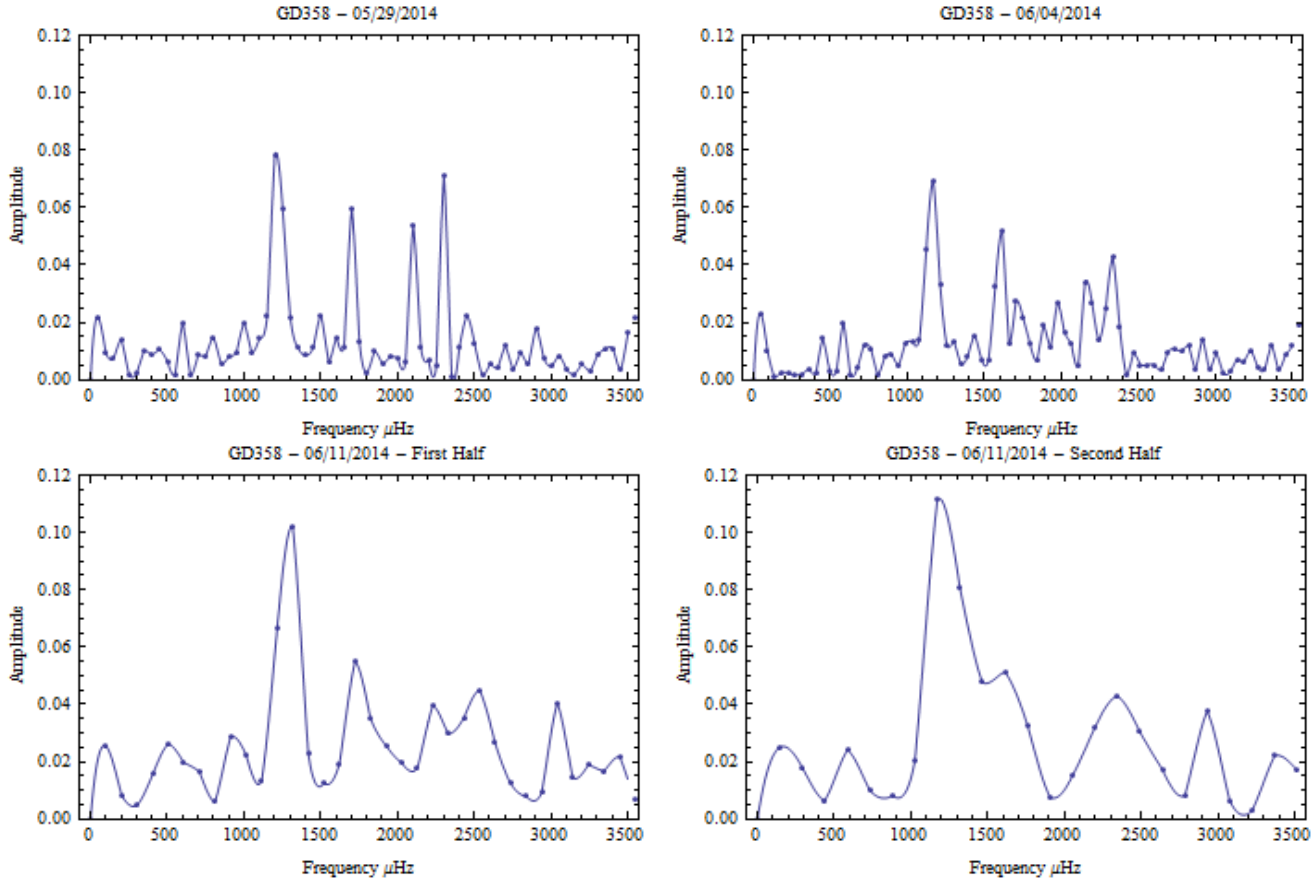

Fig. 4. Plots of frequency spectra from the three nights of data. The third night was split into two parts so that a Fourier transform could be applied. Measurements of the value of frequency at the peaks in these graphs are reported in Table 1.

VI. Conclusion

The values of frequencies from the measured power spectra were in good agreement with the published results from the WET website. Though not all of the known frequencies were identified, the uncertainty in the observed frequencies was very small. The cause of the non-inclusion of the unidentified frequencies is known, and a solution to the problem is very possible.

Because the runs of data were short, the frequency estimates were not as refined as they could have been. This project successfully supplied high quality data to the WET program, which will be able to use this data along with data from other telescopes to aid their research on pulsating white dwarfs.

VII. Acknowledgment

I thank the Central Texas Astronomical Society for allowing the use of the telescope, and especially Willie Strickland. I also thank Dr. Truell Hyde, Dr. Lorin Matthews and the Center for Astrophysics, Space Physics, and Engineering Research. This project was possible due to the National Science Foundation grand number 0847127.

VIII. References

[1] D. Koester and G. Chanmugam, "Physics of white dwarf stars," *Rep. Prog. Phys.*, vol. 53, no. 7, p. 837, Jul. 1990.

[2] S. O. Kepler, R. E. Nather, D. E. Winget, A. Nitta, S. J. Kleinman, T. Metcalfe, K. Sekiguchi, J. Xiaojun, D. Sullivan, T. Sullivan, R. Janulis, E. Meistas, R. Kalytis, J. Krzesinski, W. Ogloza, S. Zola, D. O'Donoghue, E. Romero-Colmenero, P. Martinez, S. Dreizler, J. Deetjen, T. Nagel, S. L. Schuh, G. Vauclair, F. J. Ning, M. Chevreton, J.-E. Solheim, J. M. G. Perez, F. Johannessen, A. Kanaan, J. E. Costa, A. F. M. Costa, M. A. Wood, N. Silvestri, T. J. Ahrens, A. K. Jones, A. E. Collins, M. Boyer, J. S. Shaw, A. Mukadam, E. W. Klumpe, J. Larrison, S. Kawaler, R. Riddle, A. Ulla, and P. Bradley, "The Everchanging Pulsating White Dwarf GD358," *Astronomy and Astrophysics*, vol. 401, no. 2, pp. 639–654, Apr. 2003.

[3] S. O. Kepler, E. L. Robinson, and R. E. Nather, "The light curve of the ZZ Ceti star G226-29," *The Astrophysical Journal*, vol. 271, pp. 744–753, Aug. 1983.

[4] D. E. Winget and S. O. Kepler, "Pulsating White Dwarf Stars and Precision Asteroseismology," *Annual Review of Astronomy and Astrophysics*, vol. 46, no. 1, pp. 157–199, Sep. 2008.

[5] G. Fontaine and P. Brassard, "The Pulsating White Dwarf Stars,"*Publications of the Astronomical Society of the Pacific*, vol. 120, no. 872, pp. 1043–1096, Oct. 2008.

[6] "The pulse of a white dwarf," *Sky & Telescope*, vol. 89, no. 2, p. 14, Feb. 1995.

[7] D. E. Winget, R. E. Nather, J. C. Clemens, J. L. Provencal, S. J. Kleinman, P. A. Bradley, C. F. Claver, J. S. Dixson, M. H. Montgomery, C. J. Hansen, B. P. Hine, P. Birch, M. Candy, T. M. K. Marar, S. Seetha, B. N. Ashoka, E. M. Leibowitz, D. O'Donoghue, B. Warner, D. A. H. Buckley, P. Tripe, G. Vauclair, N. Dolez, M. Chevreton, T. Serre, R. Garrido, S. O. Kepler, A. Kanaan, T. Augusteijn, M. A. Wood, P. Bergeron, and A. D. Grauer, "Whole earth telescope observations of the DBV white dwarf GD 358," *The Astrophysical Journal*, vol. 430, pp. 839–849, Aug. 1994.

[8] http://darc.physics.udel.edu/wet/damp06/phptools/index.php.

[9] P. R. Swan, "Discrete Fourier Transforms of Nonuniformly Spaced Data,"*The Astronomical Journal*, vol. 87, p. 1608, Nov. 1982.

[10] J. L. Provencal, H. L. Shipman, and Wet Team, "An Update on XCOV25: GD358," *Communications in Asteroseismology*, vol. 154, pp. 25–36, Jun. 2008.

[11] A. W. Harris and B. Warner, A Practical Guide to Lightcurve Photometry and Analysis. Springer, 2007.